



Cite this: *New J. Chem.*, 2018, 42, 19260

## Inhibition of amyloid fibril formation of $\beta$ -lactoglobulin by natural and synthetic curcuminoids†

Sanhita Maity,<sup>a</sup> Sampa Pal,<sup>a</sup> Subrata Sardar,<sup>a</sup> Nayim Sepay,<sup>ib</sup><sup>a</sup> Hasan Parvej,<sup>a</sup> Shahnaz Begum,<sup>a</sup> Ramkrishna Dalui,<sup>a</sup> Niloy Das,<sup>b</sup> Anirban Pradhan<sup>ib</sup><sup>c</sup> and Umesh Chandra Halder<sup>ib</sup><sup>\*a</sup>

The aggregation of proteins has been associated with several aspects of daily life, including food processing, blood coagulation and many neurodegenerative infections. However, the actual mechanisms responsible for amyloidosis, the irreversible fibril formation of various proteins, which is linked to disorders such as Alzheimer's disease, Creutzfeldt–Jakob disease and Huntington's disease, have not yet been fully elucidated. Curcumin, a potent anti-oxidant, exhibits anti-amyloid activity; however, its activity is limited due to its instability. Therefore, chemical modifications of curcumin have been performed to obtain molecules with enhanced stability and superior anti-amyloid activity. Herein, the main objective of this study is related to the inhibitory effects of three stable analogs of curcumin against bovine  $\beta$ -lactoglobulin ( $\beta$ -lg) fibrillization. We inferred that a pyrazole derivative of curcumin showed remarkable potency in arresting the fibrillization of  $\beta$ -lg, as revealed by biophysical techniques. Molecular docking demonstrated that pyrazole-mediated inhibition of  $\beta$ -lg fibrillogenesis may be initiated by interacting with aggregation-prone regions of the protein and preventing interactions between monomers, leading to suppression of the overall aggregation process. This work alludes to a possible broader scope for discovery of other small molecules that may exert similar effects against amyloid formation and its associated neurodegenerative diseases.

Received 27th June 2018,  
Accepted 13th October 2018

DOI: 10.1039/c8nj03194k

rsc.li/njc

## Introduction

The anomalous self-assembly and accumulation of misfolded proteins is known to have common cellular and molecular mechanisms, including protein aggregation, which is the known leading causative agent of a number of conformational diseases, such as Alzheimer's disease (AD), Parkinson's disease (PD), Huntington's disease (HD) and prion disease.<sup>1,2</sup> The aggregates consist of fibers with cross  $\beta$ -sheet structures, termed harmful 'amyloids', and their morphological features are not associated with behaviors of specific proteins. Although the proper aetiology of AD remains controversial, diverse factors appear to play vital roles in the pathophysiology of the disease; these include abnormal  $\beta$ -amyloid (A $\beta$ ) deposits in extracellular amyloid plaques, which lead to progressive neuronal death, tau protein hyperphosphorylation, metal ion

dyshomeostasis, oxidative stress, and neurotransmitter system dysfunction.<sup>3–7</sup> Different peptides and proteins generate morphologically similar or different amyloid fibrils through dimer and oligomer formation; this has been hypothesized to occur in a stepwise fashion, with a slow phase of nucleation of the precursors of the amyloid fibrils followed by a relatively fast elongation phase.<sup>8</sup> Moreover, in the formation of amyloid fibrils, the incentive to assemble arises from favorable solvation energies and side-chain interactions accompanying the formation of  $\beta$ -sheet structures.<sup>9</sup> Currently, numerous clinical and experimental studies are revealing that soluble oligomeric and protofibrillar forms of proteins are potentially neurotoxic.<sup>10,11</sup>

Recently, the most challenging research task has focused on the inhibition of fibril formation<sup>12–14</sup> by the employment of small molecules. These potent modulators are believed to stabilize monomers by blocking the formation of toxic oligomers and to divert the monomeric proteins to off-pathway non-toxic intermediates. Small molecules are being developed to inhibit aggregation of A $\beta$ ,<sup>15</sup>  $\alpha$ -synuclein<sup>16</sup> and prions.<sup>17</sup>

Much evidence has shown that polyphenols, which have structural constraints, are effective in the inhibition of amyloid fibrillation.<sup>18,19</sup> Curcumin, a classical active yellow lipid-soluble  $\beta$ -diketone dietary polyphenolic component, has been

<sup>a</sup> Organic Chemistry Section, Department of Chemistry, Jadavpur University, Kolkata 700032, India. E-mail: uhalder2002@yahoo.com

<sup>b</sup> Department of Chemistry, Durgapur Govt. College, Durgapur, West Bengal 713214, India

<sup>c</sup> Director's Research Unit (DRU), Indian Association for the Cultivation of Science, Kolkata-700032, India

† Electronic supplementary information (ESI) available. See DOI: 10.1039/c8nj03194k

extensively studied during the last few decades not only for its well-known pharmacological attributes, such as antioxidant, anticancer, antibiotic and anti-amyloidogenic properties, but also for its protective activities and intrinsic nontoxicity.<sup>20</sup> Curcumin has been found to non-specifically bind to amyloid- $\beta$  monomers and fibrils and modify protein aggregation pathways.<sup>21</sup> Despite its extensive bioactivities, the potential efficacy of curcumin is extremely limited for the prevention of aggregation-related diseases due to its moderate bioavailability and poor potency related to its insolubility in water as well as its poor absorption and metabolic instability.<sup>22</sup> Many recent studies have focused on the generation of rationally designed curcumin analogues and derivatives which have been demonstrated to have very promising potency and bioactivity compared to curcumin against amyloid proteins *in vitro* as well as *in vivo*.<sup>23</sup>

Bovine  $\beta$ -lactoglobulin ( $\beta$ -lg), a well-known globular major whey protein comprising 162 amino acids with a molecular mass of 18.3 kDa, is predominantly a  $\beta$ -sheet protein.<sup>24</sup> In addition,  $\beta$ -lg possesses two intramolecular disulphide bonds (Cys<sub>66</sub>-Cys<sub>160</sub>, Cys<sub>106</sub>-Cys<sub>119</sub>) and one free thiol group (Cys<sub>121</sub>) which is buried between the  $\beta$ -barrel and the major  $\alpha$ -helix.<sup>25</sup> Bovine  $\beta$ -lg is an extensively used model carrier protein for hydrophobic ligands due to its pH-dependent opening, excellent encapsulating properties and unique resistivity to acidic pH.<sup>26</sup> Due to its carrier properties, this protein is a good candidate to serve as a model transporter for delivering important hydrophobic nutrients to improve their bioavailability. The protein  $\beta$ -lg presents an interesting conundrum because it forms fibrillar structures upon thermal treatment at physiological pH.<sup>27,28</sup> Despite the increasing quantity of studies on this topic, the mechanisms of fibril formation and identification of the building blocks of fibrils is still a subject of debate.<sup>29</sup> The primary cause of initiation of thermal aggregation of  $\beta$ -lg is thought to involve disulfide bridge formation by exchange between free cysteine and one of the two disulfide bridges.<sup>30</sup> A two-step model has been proposed for the aggregation process at neutral pH, in which small particles are formed first and then further aggregate into large clusters that exhibit self-similarity in certain cases.<sup>31</sup>

A recent proposal by Ma *et al.* suggests involvement of the lag time for the formation of stable nuclei (nucleation) and the apparent rate constant for the growth of fibrils (elongation) in the kinetics of the fibrillation process at neutral pH.<sup>32</sup> However, the aggregation process usually involves conformational changes of the whole protein or of a specific domain; this is often attributed to the association of partially unfolded molecules.<sup>33</sup> Extensive research has been carried out to establish the mode of action of curcumin and the chemical moiety responsible for its anti-fibrillogenic properties; however, the actual mechanism responsible for these activities remains elusive due to the instability of curcumin in solution. Moreover, efforts to explore the potency of stable curcumin analogues as inhibitors of  $\beta$ -lg aggregation are lacking. Herein, we therefore screened curcumin derivatives, isosteric isoxazoles (IOC), pyrazoles (PY) and curcumin diacetate (DAC) (Fig. 1), as ideal small molecular candidates to achieve better pharmacological attributes against  $\beta$ -lg aggregation *in vitro*. Pyrazole (PY) and isoxazole (IOC) derivatives have also

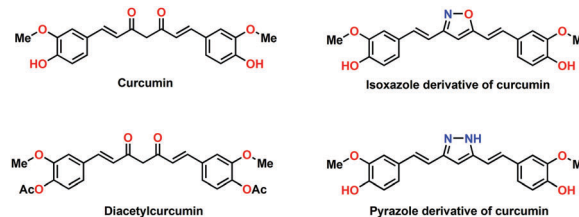


Fig. 1 Chemical structures of curcumin and its derivatives.

been used as potent ligands of fibrillar A $\beta$ -42 aggregates<sup>34</sup> and also have the ability to prevent tubulin self-assembly.<sup>35</sup> It has been reported that curcumin diacetate (DAC) also has an influence on hIAPP aggregation.<sup>23</sup> However, by employing several biophysical techniques, for the first time, we have evaluated the effects of curcumin derivatives on the inhibitory mechanism of  $\beta$ -lg fibril formation *in vitro*.

## Results and discussion

### SDS-polyacrylamide gel electrophoresis study

SDS-PAGE analysis is a convenient technique to observe protein aggregation under non-reducing conditions. In the SDS-PAGE study, the native  $\beta$ -lg appeared as a single band (Lane 2) in the gel around 18.3 kDa, which corresponds to the monomeric state of  $\beta$ -lg. The  $\beta$ -lg sample in Fig. 2A was incubated at 75 °C in 10 mM phosphate buffer at pH 7.4 for 6 h; a series of protein bands appeared, suggesting the highly packed nature of the aggregates formed after incubation (Lane-3). This useful technique was employed to dissociate all the non-covalently bonded aggregates into monomers while the disulphide-linked aggregates remained intact. The thiol group of cys<sub>121</sub> of  $\beta$ -lg forms S-S linkages when incubated at 75 °C to 80 °C, which is associated with the formation of dimers and other covalently bound “intermediates” during aggregation<sup>48,49</sup> by scrambling of disulphide bonds (creation of new intramolecular and intermolecular disulphide bridges and rearrangement of existing intramolecular disulphide bridges).<sup>50</sup>

When  $\beta$ -lg was incubated at 75 °C for 6 h, bands appeared in the gel corresponding to the formation of self-assemblies of  $\beta$ -lg (Lane 3, bands II-V) and to the monomer, with lower intensity (Lane 3, band I). The SDS-PAGE analysis of heat-treated  $\beta$ -lg in the presence of curcumin derivatives at a molar concentration ratio of 1:1 under non-reducing conditions showed a very different result. In the presence of curcumin and DAC (Lane 6 and Lane 7) at molar concentration ratios of 1:1, trimeric states were also formed. Stabilization of the dimeric state with a less intense band in the trimeric state was observed when  $\beta$ -lg was incubated with the IOC derivative at a molar concentration ratio of 1:1 (Lane 4). The dimeric state of  $\beta$ -lg was stabilized in the presence of PY derivative (Lane 5) at a molar concentration ratio of 1:1; this is consistent with its lower electrophoretic mobility. The stabilization of the dimeric state by the PY derivative may be due to blocking of the formation of toxic oligomers and prevention of the primary nucleation process to destabilize the formation of oligomers of  $\beta$ -lg.

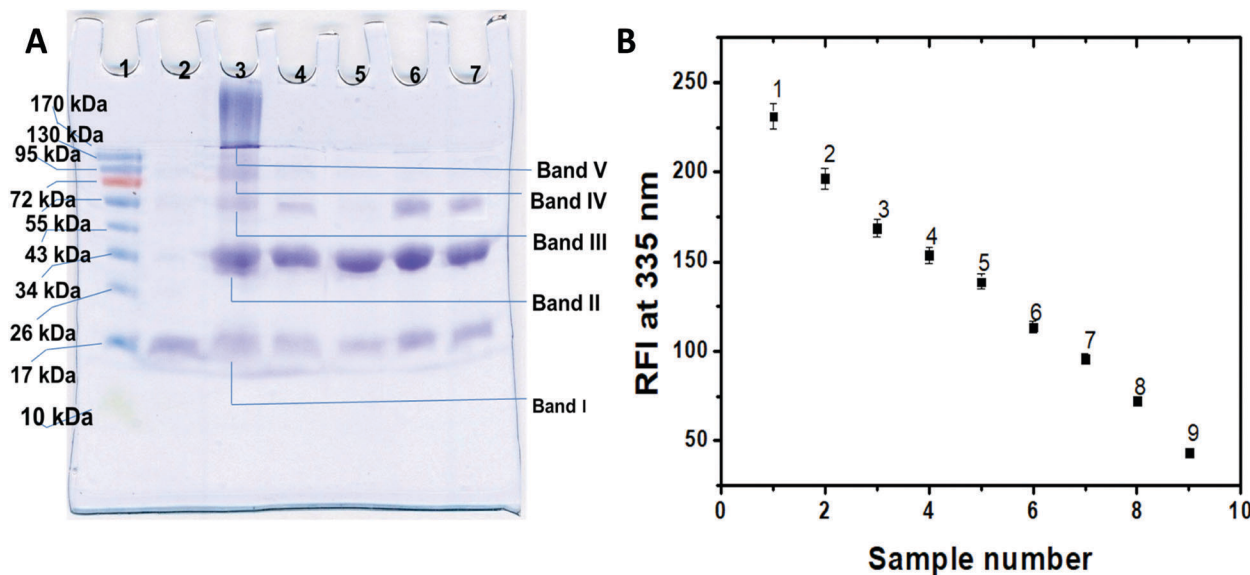


Fig. 2 (A) SDS-PAGE (12%) patterns of native  $\beta$ -lg (Lane 2) and  $\beta$ -lg incubated at 75 °C for 6 h in the absence (Lane 3) and presence of 1:1 molar concentration ratios of IOC (Lane 4), PY (Lane 5), curcumin (Lane 6) and DAC (Lane 7). Lane 1 represents the SDS PAGE pattern of marker proteins with known molecular weights (Page Ruler™, Prestained Protein Ladder, 10, 17, 26, 34, 43, 55, 72, 95, 130 and 170 kDa, respectively; Fermentus Life Science, #SM0671) run parallel. (B) Relative fluorescence intensities of tryptophenyl residues (emitted at 335 nm) of  $\beta$ -lg incubated at 75 °C for 6 h in the absence (1) and presence of curcumin (2, 3), DAC (4, 5), IOC (6, 7) and PY (8, 9) at molar concentration ratios of 1:0.5 and 1:1, respectively in 10 mM phosphate buffer at pH 7.4 containing 2% ethanol. The samples were excited at 295 nm and the emission was recorded in the range of 310 to 400 nm. The protein concentrations during intrinsic fluorescence were 13.6  $\mu$ M. The results are the mean of three different experiments performed in duplicate. Standard deviations are within the range of  $\pm 2.0$ .

Lane 1 represents the SDS-PAGE pattern of marker proteins with known molecular weights (Page Ruler™, Prestained Protein Ladder, 10, 17, 26, 34, 43, 55, 72, 95, 130, and 170 kDa, respectively; Fermentus Life Science, #SM0671) run parallel.

### Tertiary conformational alterations probed by tryptophan fluorescence

Intrinsic fluorescence parameters, such as fluorescence intensity (FI) and emission maxima ( $\lambda_{\text{max}}$ ), provide a very sensitive mean for studying the structural dynamics and polarity of protein chromophores, *viz.* Trp, Tyr and Phe. The two tryptophan residues of  $\beta$ -lg, Trp<sub>19</sub> and Trp<sub>61</sub> provide a convenient spectroscopic means for assessing the conformational states of proteins. In particular, Trp<sub>61</sub> is quenched by the close proximity of the neighbouring disulphide bond, Cys<sub>160-66</sub>, and Trp<sub>19</sub> is situated within the centre of the hydrophobic calyx of the protein in the native state.<sup>51</sup> Trp<sub>19</sub> was therefore the most useful probe for tryptophan fluorescence of bovine  $\beta$ -lg. In our study, the  $\beta$ -lg incubated at pH 7.4 exhibited a prominent emission peak around 335 nm in the wavelength range of 300 to 400 nm when excited at 295 nm. Hence, the relative changes in the fluorescence intensity around 335 nm can be used as a probe for changes in the microenvironment in the vicinity of the tryptophan residues of proteins arising due to altered conformations. Fig. 2B reveals the relative fluorescence intensities at 335 nm of  $\beta$ -lg after co-incubation with curcumin, DAC, IOC and PY derivatives at molar concentration ratios of 1:0.5 and 1:1 for 6 h at 75 °C. The maximal quenching of the fluorescence intensity (Fig. 2B) of  $\beta$ -lg was observed in the

presence of PY derivative (Fig. 2B, circle 9) at a 1:1 molar concentration. The decreases in the intrinsic fluorescence intensity suggest that curcumin, DAC, IOC and PY derivatives interacted with  $\beta$ -lg, resulting in conformational changes of the protein; PY derivative caused the maximal change in the protein conformation.

### Disassembly of $\beta$ -lg aggregates with curcumin derivatives monitored by ThT assay

The thioflavin T (ThT) assay is believed to be a reliable technique for quantification of amyloid fibrils; therefore, we monitored the changes in dye fluorescence to investigate the inhibitory effects of these derivatives against  $\beta$ -lg aggregation *in vitro*. All the samples were blank corrected (data not shown) because coloured compounds can suppress ThT fluorescence; also, we considered the percent increase in ThT intensity instead of the absolute intensities. The extent of aggregation was monitored by sampling at regular intervals. Fig. 3A shows the kinetics of  $\beta$ -lg aggregation in the absence and presence of curcumin derivatives monitored by ThT binding assay. The percentage increases in ThT fluorescence for all the compounds were calculated using eqn (1). The kinetic curves of the ThT fluorescence intensity at 485 nm are consistent with a nucleation-dependent polymerization model in which the lag corresponds to the nucleation phase and the exponential part corresponds to the elongation phase (fibril growth).<sup>32</sup> In our experimental conditions, aggregated  $\beta$ -lg displayed a lag phase of  $\sim 150$  min (Fig. 3A). The significantly decreased ThT fluorescence for PY derivative indicates that it suppressed fibril

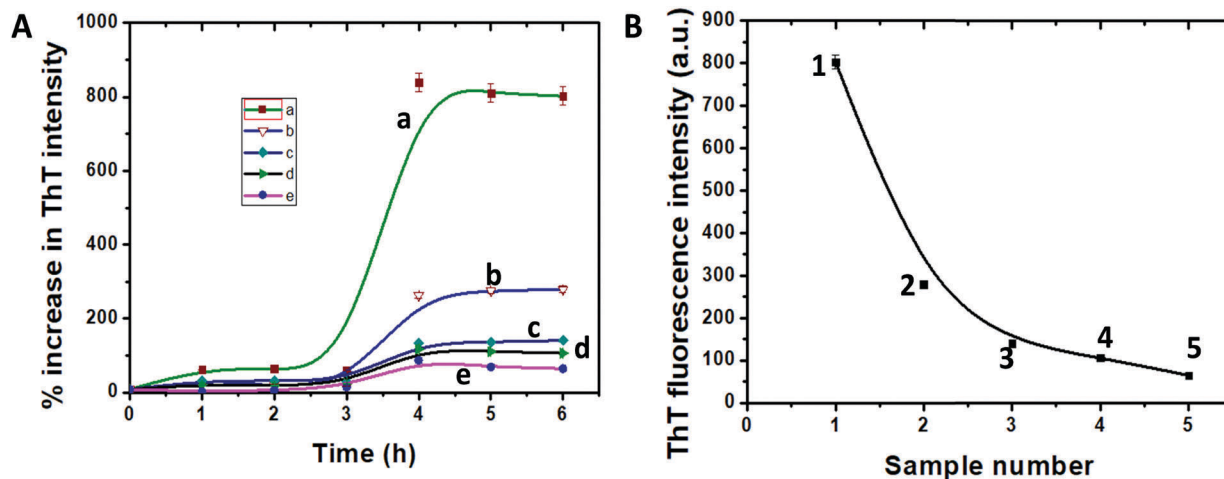


**Fig. 3** (A) Time course of  $\beta$ -Ig aggregation in the absence (curve a) or presence of curcumin derivatives as monitored by ThT assay.  $\beta$ -Ig was co-incubated at 75 °C with curcumin (curve b), DAC (curve c), IOC (curve d) and PY (curve e) at molar concentration ratios of 1 : 1 for 6 hours in 10 mM phosphate buffer at pH 7.4 containing 2% ethanol. The ability of these compounds to prevent aggregation is shown as the percentage increase in ThT fluorescence intensity. Aggregated samples were incubated with 50  $\mu$ M of ThT for 30 min at 25 °C. The samples were excited at 440 nm and the emissions were recorded at 485 nm. The results are the mean of three different experiments. (B) The dose–response curve plotting the plateau value of the ThT fluorescence intensities estimated from the time course of aggregated  $\beta$ -Ig sample alone (1) and co-incubated with curcumin (2), DAC (3), IOC (4) and PY (5) derivatives. The data are the average of at least three independent experiments. Error bars are given within the range of  $\pm 2.0$ . The protein concentration during the ThT assay was 13.6  $\mu$ M.

formation of  $\beta$ -Ig compared to the other derivatives; the order of the inhibitory potentials of the compounds was observed to be PY > IOC > DAC > curcumin. This can be attributed to the stabilization of low molecular weight (LMW) oligomers or dimers by the pyrazole form of curcumin; the stabilized species did not consequently form  $\beta$ -sheet-rich fibrillar species.

#### Detection of exposed hydrophobic clusters by ANS binding

The exposure of the contiguous hydrophobic surface areas of folding intermediates is detected through 1-anilino-8-naphthalene sulfonate (ANS) binding, the most commonly utilized fluorescence probe for detecting the non-polar character of proteins.<sup>52</sup> ANS did not significantly bind to  $\beta$ -Ig in its native state, indicating the absence of exposed hydrophobic pockets.

It was reported that ANS is practically non-fluorescent in water but produces brilliant fluorescence with an emission maximum from 510 nm to 480 nm upon binding to hydrophobic patches of proteins.<sup>53</sup> As expected, the spectrum of native  $\beta$ -Ig showed negligible ANS fluorescence (Fig. 4B, profile a). In the absence of curcumin derivatives, the thermally incubated  $\beta$ -Ig at pH 7.4 showed maximum ANS fluorescence intensity at 480 nm with a blue shift of the emission. This enhancement of fluorescence intensity can be attributed to the increased access of ANS to the hydrophobic patches present in proteins upon thermal incubation compared to native  $\beta$ -Ig. These hydrophobic patches increase the protein–protein interactions, leading to thermal aggregation of  $\beta$ -Ig.<sup>54</sup> However, in the presence of curcumin and its potential analogs, during thermal exposure of  $\beta$ -Ig, significant decreases of the ANS fluorescence intensity were observed, indicating a loss of ANS binding sites. Fig. 4B suggests that a gradual decrease of ANS fluorescence intensity was observed for DAC (profile e and profile f) at molar concentration

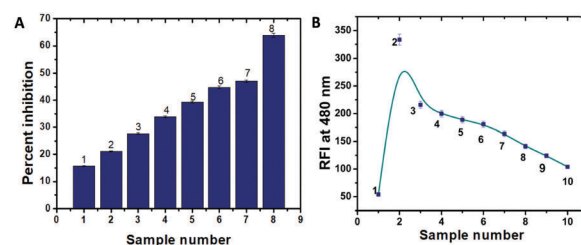


**Fig. 4** (A) Percentage inhibition of aggregation of  $\beta$ -Ig by curcumin and curcumin derivatives as observed by ThT assay.  $\beta$ -Ig was co-incubated at 75 °C with curcumin (1, 2), DAC (3, 4), IOC (5, 6) and PY (7, 8) at 1 : 0.5 and 1 : 1 molar concentrations, respectively, for 6 h in 10 mM phosphate buffer at pH 7.4 containing 2% ethanol. The percentage of inhibitory effects of these compounds was calculated using eqn (2). (B) ANS fluorescence of native  $\beta$ -Ig (line a) and  $\beta$ -Ig incubated at 75 °C for 6 h in the absence (line b) and presence of curcumin (line c, line d), DAC (line e, line f), IOC (line g, line h), and PY (line i, line j) at molar concentration ratios of 1 : 0.5 and 1 : 1, respectively, in 10 mM phosphate buffer at pH 7.4 containing 2% ethanol. (inset) Relative fluorescence intensities at 480 nm of native  $\beta$ -Ig (1) and incubated  $\beta$ -Ig at 75 °C for 6 h in the absence (2) and presence of curcumin (3, 4), DAC (5, 6), IOC (7, 8), PY (9, 10) at molar concentration ratios of 1 : 0.5 and 1 : 1, respectively in 10 mM phosphate buffer at pH 7.4 containing 2% ethanol. The concentration of  $\beta$ -Ig was maintained at 13.6  $\mu$ M. Fluorescence emissions were monitored in the wavelength range of 460 to 600 nm after excitation at 380 nm. Results are the average of triplicate measurements. The protein concentration during the ANS fluorescence studies was 13.6  $\mu$ M. Standard deviations are within the range of  $\pm 2.0$ .

ratios of 1 : 0.5 and 1 : 1 with respect to the same molar concentrations of curcumin (profile c and profile d). A gradual decrease of ANS fluorescence intensity was observed during thermal co-incubation of  $\beta$ -Ig with the IOC derivative at molar concentration ratios of 1 : 0.5 and 1 : 1 (Fig. 4B, profile g and profile h).

In contrast, no significant ANS binding was observed upon thermal co-incubation of  $\beta$ -lg with PY derivative at a molar concentration ratio of 1:1 (Fig. 4B, profile j). The decreased ANS binding in the presence of the curcumin derivatives suggests the formation of fewer hydrophobic patches by  $\beta$ -lg upon thermal stress at 75 °C. Fig. 4B shows the relative fluorescence intensities (RFI) at 480 nm of native  $\beta$ -lg and  $\beta$ -lg incubated at 75 °C for 6 h in the absence and presence of curcumin and curcumin derivatives. The decreased ANS binding in presence of the curcumin derivatives is highly consistent with the lower population of partially folded intermediates; thus, these derivatives are capable of suppressing  $\beta$ -lg aggregation.

### Monitoring the disaggregation of $\beta$ -lg utilizing Rayleigh light scattering (RLS) measurements

Rayleigh light scattering (RLS) is one of the most commonly used experiments in the arena of protein aggregation. The utilization of RLS data is based upon the principle that increased RLS intensity of a protein solution is an indication of aggregation. Conventionally, a decrease of RLS intensity is a useful parameter to support the disaggregation or disassembly of proteins. Thus, Fig. 5A shows the changes in the scattering intensity measured at 350 nm after exciting heat-treated  $\beta$ -lg solution at 350 nm in the absence and presence of varying amounts of the aforementioned curcumin derivatives at pH 7.4. It was noted that the maximum scattering intensity was observed for incubated  $\beta$ -lg, suggesting aggregate formation. Furthermore, when DAC and IOC were used at molar concentration ratios of 1:0.5 and 1:1, respectively, significant decreases in the scattering intensity were observed with respect to curcumin at same concentration level. In particular, a

remarkable decrease in scattering intensity was noted in the presence of PY derivative at a molar concentration of 1:1. Control measurements with the aforementioned molar concentrations of the curcumin derivatives were performed and compared. Higher concentrations of curcumin derivatives scattered UV light at 350 nm. Hence, the decrease in scattering intensity in the presence of PY derivative at a molar concentration ratio of 1:1 indicates that this derivative has an appreciable potential inhibitory effect to decrease the self-assembly of  $\beta$ -lg aggregations.

### Quantifications of amyloid formation employing Congo red (CR) measurements

To validate the findings of the ThT assay, the inhibition of  $\beta$ -lg aggregation was also confirmed by the Congo red (CR) binding assay. Depending on the state of protein aggregation, CR binding to the extensive  $\beta$ -sheet structures is expected to cause an increase in absorption, with a bathochromic shift in its characteristic absorption spectrum (from approximately 490 nm unbound to 500 nm bound). The CR spectral shift assay potentially enables quantification of amyloid fibrils, where coloured compounds interfere with ThT fluorescence.<sup>55</sup> Generally, at neutral pH,  $\beta$ -lg showed absorption maxima at 493 nm (Fig. 5B, profile a) and the thermally incubated  $\beta$ -lg showed absorption maxima at 500 nm, accompanied with broadening of the areas of absorbance. This is attributed to the confinement of the CR dye in the clusters of the  $\beta$ -sheet peptide backbones of the aggregates. We observed that the increased peak shift detected in aggregated  $\beta$ -lg was not visible in the spectra of  $\beta$ -lg samples containing curcumin and its derivatives, corroborating the results of the ThT binding assay. In the presence of curcumin, DAC and IOC derivatives at molar concentration ratios of 1:0.5 and 1:1, the

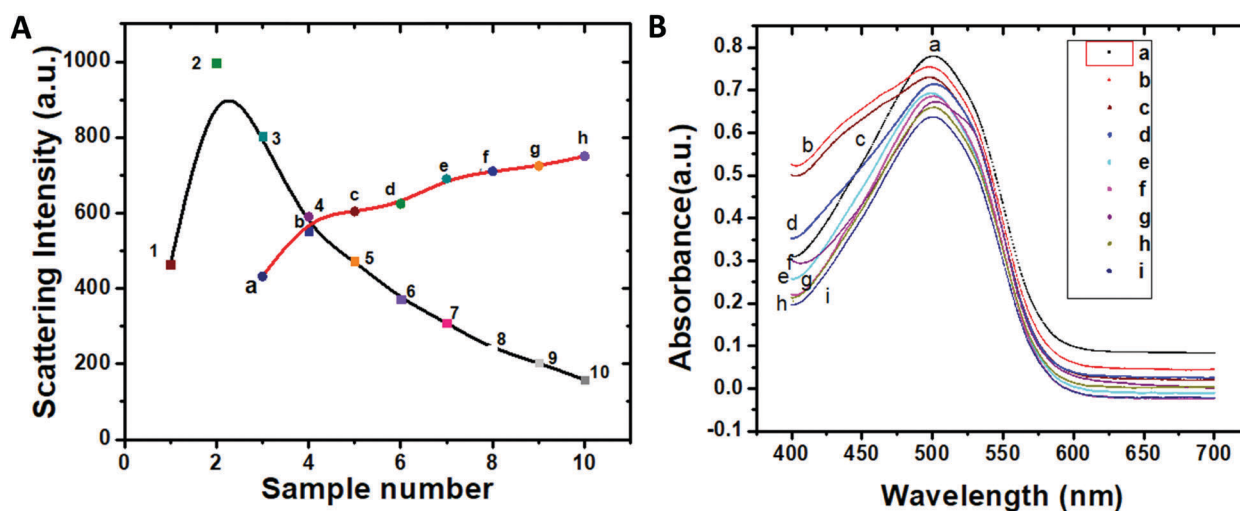


Fig. 5 (A) Rayleigh light scattering data of native  $\beta$ -lg (1) and  $\beta$ -lg incubated at 75 °C for 6 h in the absence (2) and presence of curcumin (3, 4), DAC (5, 6), IOC (7, 8), and PY (9, 10) at molar concentration ratios of 1:0.5 and 1:1, respectively, in 10 mM phosphate buffer at pH 7.4 containing 2% ethanol. Control measurements with curcumin derivatives are shown in circles: [circle a – curcumin (13.6  $\mu$ M), circle b – curcumin (27  $\mu$ M), circle c – DAC (13.6  $\mu$ M), circle d – DAC (27  $\mu$ M), circle e – IOC (13.6  $\mu$ M), circle f – IOC (27  $\mu$ M), circle g – PY (13.6  $\mu$ M), and circle h – PY (27  $\mu$ M)]. The samples were excited and emitted at 350 nm. (B) Congo red assay of native  $\beta$ -lg (line a) and  $\beta$ -lg incubated at 75 °C for 6 h in the absence of curcumin (line c, line d), DAC (line e, line f), IOC (line g, line h), and PY (line i, line j) at molar concentration ratios of 1:0.5 and 1:1, respectively, in 10 mM phosphate buffer at pH 7.4 containing 2% ethanol. Absorbance was scanned in the wavelength range of 400 nm to 700 nm using a UV-Vis spectrophotometer. Results are the mean of three different experiments. The protein concentration was maintained at 27.2  $\mu$ M.

absorbance decreased with respect to the degree of inhibition of amyloid fibril formation of  $\beta$ -lg. The lowest absorbance for PY derivative at a molar concentration ratio of 1:1 may be due to entanglement of the formed fibrils into relatively unordered smaller aggregates (Fig. 5B, profile j). It was confirmed that PY derivative at a molar concentration (1:1), stabilizes the dimeric form of the protein to a greater extent, inhibiting nucleation and elongation for the formation of higher aggregates.

### Dynamic light scattering (DLS) study to investigate amyloid fibrillation of $\beta$ -lg

Dynamic light scattering (DLS) studies are frequently employed to measure the hydrodynamic radii of spherical particles in solution, and the intensity of scattered light is dominated by the large particles present in the solution.<sup>56</sup> Although the  $\beta$ -lg aggregates are heterogeneous, either spherical or rod-like fibrous shapes, DLS data analysis can provide quantitative estimations of the size distributions in the presence of curcumin derivatives. Fig. 6A shows that the hydrodynamic radius of native  $\beta$ -lg ranges from 25 nm to 100 nm (profile a). During thermal incubation at 75 °C, the monomers of  $\beta$ -lg aggregated in an oligomeric state and formed a new population of particles, increasing the particle size by 5-fold (sizes ranging from 25 nm to 500 nm) (Fig. 6A, profile b). The data were plotted as the scattered light intensity *versus* the radius in nm. Notably, the presence of higher ordered aggregates indicates that the aggregates are formed from  $\beta$ -lg dimers (possibly in equilibrium with monomers) with involvement of multimers, such as tetramers and pentamers. From the experimental point of view, when  $\beta$ -lg was co-incubated with curcumin at 75 °C for 6 h at a molar concentration ratio of 1:1 (Fig. 6A, profile d), the sizes (ranging from 25 nm to 360 nm) of the aggregates decreased to a greater extent than at a molar concentration ratio of 1:0.5 (sizes ranging from 25 nm to 475 nm) (Fig. 6A, profile c).

It should also be pointed out that in presence of DAC at a molar concentration ratio of 1:1 (Fig. 6A, profile f), the sizes (ranging from 25 nm to 350 nm) of the aggregates decreased with respect to curcumin at the same concentration level. However, in the presence of IOC at a molar concentration ratio of 1:1, the scattering was dominated by smaller particles (size ranging from 25 nm to 320 nm) (Fig. 6A, profile h). Specifically, a drastic change in the size distribution of large  $\beta$ -lg particles (aggregates) was observed upon thermal co-incubation with PY derivative at a molar concentration ratio of 1:1 (size ranging from 25 nm to 260 nm) (Fig. 6A, profile j). The hydrodynamic radius data suggest the apparent quenching of aggregate growth which encompasses the association of protein molecules, probably due to the formation of compact dimers in the presence of PY derivative. Our DLS data correlates with the SDS-polyacrylamide gel electrophoresis observations.

### CD spectroscopy to monitor the secondary structural changes of $\beta$ -lg

Far-UV CD spectroscopy was exploited to monitor the secondary structural changes of  $\beta$ -lg in the presence of curcumin derivatives at molar concentration ratios of 1:0.5 and 1:1 at pH 7.4. The native  $\beta$ -lg shows a negative signal around 216 nm, which is characteristic of the  $\beta$ -sheet structure of  $\beta$ -lg, with a very small minimum at 207 nm, which also indicates some  $\alpha$ -helical structures (Fig. 6B, profile a).<sup>57</sup> As shown in Fig. 6B, circular dichroism (CD) experiments revealed the expected increase in the random coil/ $\beta$ -sheet conformation transition of  $\beta$ -lg after incubation at 75 °C for 6 h (Fig. 6B, profile b). This transition of the conformation is accompanied by a decrease in the  $\alpha$ -helical content of the protein structure, indicating the possibility of formation of crosslinked  $\beta$ -sheet structures. However, the thermal exposure of the protein in the presence of curcumin at a molar concentration ratio of 1:0.5 displays a significant decrease in intensity, with shifts in the band positions similar to those of the native protein (Fig. 6B, profile c). However, in the presence of curcumin at a molar concentration ratio of 1:1, the peak positions shifted to 214 nm and 209 nm (Fig. 6B, profile d). The shifting of the peak positions signifies that a conformational transition of  $\beta$ -lg from a  $\beta$ -sheet state to a physiological unfolded random coil state occurs in the presence of curcumin. In contrast, during thermal co-incubation of  $\beta$ -lg with DAC at a molar concentration ratio of 1:1, minima at 209 and 219 nm were observed (Fig. 6B, profile f). On the other hand, during thermal co-incubation of  $\beta$ -lg with IOC derivative at a molar concentration ratio of 1:1, the  $\beta$ -sheet to random coil conformation transition became dominant, indicating a loss of the gross  $\beta$ -sheet structure (Fig. 6B, profile h). In particular, in the presence of PY derivative at a 1:1 molar concentration ratio, there was a concomitant increase in the  $\alpha$ -helical structure, as evidenced by increases in ellipticity at 208 nm and 220 nm, respectively. It is of interest to note that at a molar concentration ratio of 1:1, PY showed a more pronounced helical conformation compared to the other curcumin derivatives (Fig. 6B, profile j). In this light, it can be assumed that a selective  $\beta$ -lg intermediate species was stabilized through interactions with this particular curcumin derivative. This may occur through

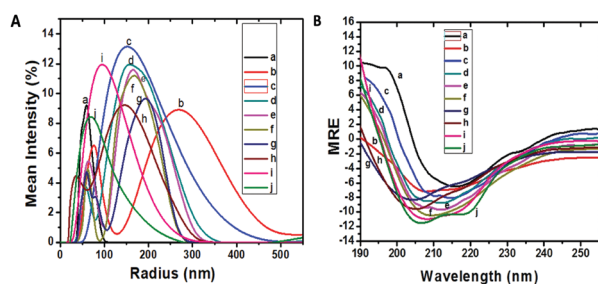


Fig. 6 (A) Number particle size distribution spectra in DLS studies of native  $\beta$ -lg (profile a) and  $\beta$ -lg incubated at 75 °C for 6 h in the absence (profile b) and presence of curcumin (profile c, profile d), DAC (profile e, profile f), IOC (profile g, profile h), and PY (profile i, profile j) at molar concentration ratios of 1:0.5 and 1:1, respectively in 10 mM phosphate buffer at pH 7.4 containing 2% ethanol. Each spectrum is an average of 48 scans. The protein concentration was maintained at 54.3  $\mu$ M. (B) Far UV-CD spectra of native  $\beta$ -lg (profile a) and  $\beta$ -lg incubated at 75 °C for 6 h in the absence (profile b) and presence of curcumin (profile c, profile d), DAC (profile e, profile f), IOC (profile g, profile h), and PY (profile i, profile j) at 1:0.5 and 1:1 molar concentration ratios, respectively in 10 mM phosphate buffer at pH 7.4 containing 2% ethanol. The concentrations of the  $\beta$ -lg samples in the far UV-CD measurements were 13.6  $\mu$ M.

charge-charge interactions between PY derivative and  $\beta$ -lg; these interactions may force the protein to attain a specific conformation, thus altering its aggregation properties rather than disrupting the helix to force aggregation of  $\beta$ -lg. To further assess the curcumin derivative-induced structural transitions, the individual secondary structural elements were analyzed with CDNN 2.1 software, and the results are shown in Table S1 (ESI<sup>†</sup>).

### FTIR study to assess secondary structural changes during $\beta$ -lg fibrillation in the presence of curcumin derivatives

Fourier transform IR (FTIR) spectroscopy is one of the most powerful spectroscopic tools for determining the secondary structures of proteins in solution and has been utilized as an independent technique for decades to confirm or refute CD measurements.<sup>37</sup> The main advantage of this approach in comparison with CD is that FTIR is much more sensitive to  $\beta$ -structures.<sup>37</sup> Information about the secondary structures of proteins can be obtained from the study of the amide I (1500–1700  $\text{cm}^{-1}$ ) band in the ATR-FTIR spectra. Fig. 7 shows the FTIR spectra of  $\beta$ -lg samples (native and thermally incubated in the absence and presence of curcumin derivatives) in  $\text{D}_2\text{O}$ -buffer. As a  $\beta$ -sheet rich protein,  $\beta$ -lg has a characteristic peak at around 1634  $\text{cm}^{-1}$  in its amide I contour, which corresponds to intramolecular  $\beta$ -sheet structures.<sup>58</sup> At elevated temperature, the peak shifts from 1634  $\text{cm}^{-1}$  to 1624  $\text{cm}^{-1}$  (Fig. 7, profile b). As a blue sheet rich protein,  $\beta$ -lg has a characteristic peak at around 1634  $\text{cm}^{-1}$  in its amide I contour, which corresponds to intramolecular shifting of the  $\beta$ -sheet band in the protein FTIR spectra, consistent with the presence of intermolecular (rather than intramolecular)  $\beta$ -sheet structures, and is the hallmark of amyloid-like fibril formation.<sup>37</sup> In the presence of curcumin at a molar concentration ratio of 1:0.5, Fig. 7 shows a shifting of the amide I band to  $\sim 1636 \text{ cm}^{-1}$ ,

indicating that there were no significant structural changes of  $\beta$ -lg (Fig. 7, profile c). However, in the presence of curcumin at a molar concentration ratio of 1:1, the amide I band shifted to  $\sim 1639 \text{ cm}^{-1}$ , indicating a  $\beta$ -sheet to random coil structural transition of  $\beta$ -lg (Fig. 7, profile d). However,  $\beta$ -lg acquired a random coil-like structure in the presence of DAC at a molar concentration ratio of 1:0.5, where the amide-I band was centered at  $\sim 1640 \text{ cm}^{-1}$  (Fig. 7, profile e). In addition, in the presence of DAC at a molar concentration ratio of 1:1, the amide I band shifted to  $\sim 1643 \text{ cm}^{-1}$ , indicating increased accessibility of random coil structures with consequent small increase in the  $\alpha$ -helical content of  $\beta$ -lg (Fig. 7, profile f). Specifically, more random coil structures were obtained when the protein was incubated with IOC derivative at molar concentration ratios of 1:0.5 and 1:1, respectively (Fig. 7, profile g and profile h). Interestingly, shifting of the amide-I band to 1653  $\text{cm}^{-1}$ , which corresponds to the preferable  $\alpha$ -helical conformation, was obtained by  $\beta$ -lg when incubated with PY derivative at a molar concentration ratio of 1:1 (Fig. 7, profile j). The FTIR data adequately support the results from the CD measurements. This led us to speculate that more inhibitory ability is exerted by PY derivative with respect to the aforementioned curcumin derivatives.

### The effects of curcumin derivatives on fibril morphology

To gain more insight, atomic force microscopy was also employed; it has been proved to be a powerful tool in the study of fibril formation.<sup>59</sup> AFM analysis was performed to visualize the extent of disruption of  $\beta$ -lg samples aggregated alone or with curcumin derivatives at molar concentration ratios of 1:1. It has been proposed that only short and curly aggregates are formed at high pH (higher than the isoelectric point, *e.g.*,  $\text{pH} > 7$ ).<sup>26</sup> The AFM image of fibrils (Fig. 8, image b) grown at  $\text{pH} 7.4$  and  $75^\circ\text{C}$  is different from those at lower protein concentrations. With higher concentrations, more numerous and mature fibrils can be obtained; therefore, in our studies, the concentration of  $\beta$ -lg was maintained at  $543 \mu\text{M}$ . To investigate the formation of  $\beta$ -lg fibrils, time-dependent transformation into fibrils was monitored by incubating  $\beta$ -lg samples at  $75^\circ\text{C}$  for 6 h and 24 h. During incubation for 6 h at  $75^\circ\text{C}$ , the monomers of  $\beta$ -lg swelled and deformed, forming aggregates. At this stage, the aggregates consisted of thicker filaments, and a protofibril-like appearance was observed (Fig. 8, image a). These protofibrils were assumed to be precursors for the formation of longer fibrils. Upon prolonged incubation at 24 h, subunits of well-developed fibrils are formed. However, filaments were no longer observed, and elongated fibrillar aggregates with apparent diameters of 140 to 150 nm formed (Fig. 8, image c). When a  $\beta$ -lg sample was co-incubated at  $75^\circ\text{C}$  for 24 h in the presence of curcumin at a molar concentration ratio of 1:1, the number and sizes of the fibrils (diameter  $\sim 120$  to  $130 \text{ nm}$ ) decreased on the mica surface, accompanied by the formation of smaller globular particles with fibrillar morphologies (Fig. 8, image e). Morphologically fragmented worm-like fibrils with diameters  $\sim 100$  to  $110 \text{ nm}$  formed when a  $\beta$ -lg sample was co-incubated in the presence of DAC (Fig. 8, image g). Furthermore, the matured fibrils were split

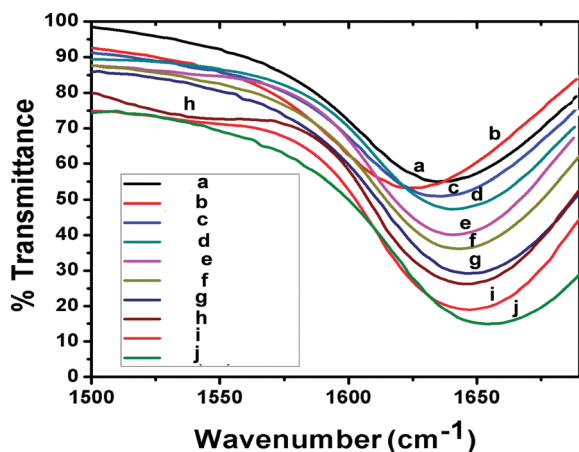
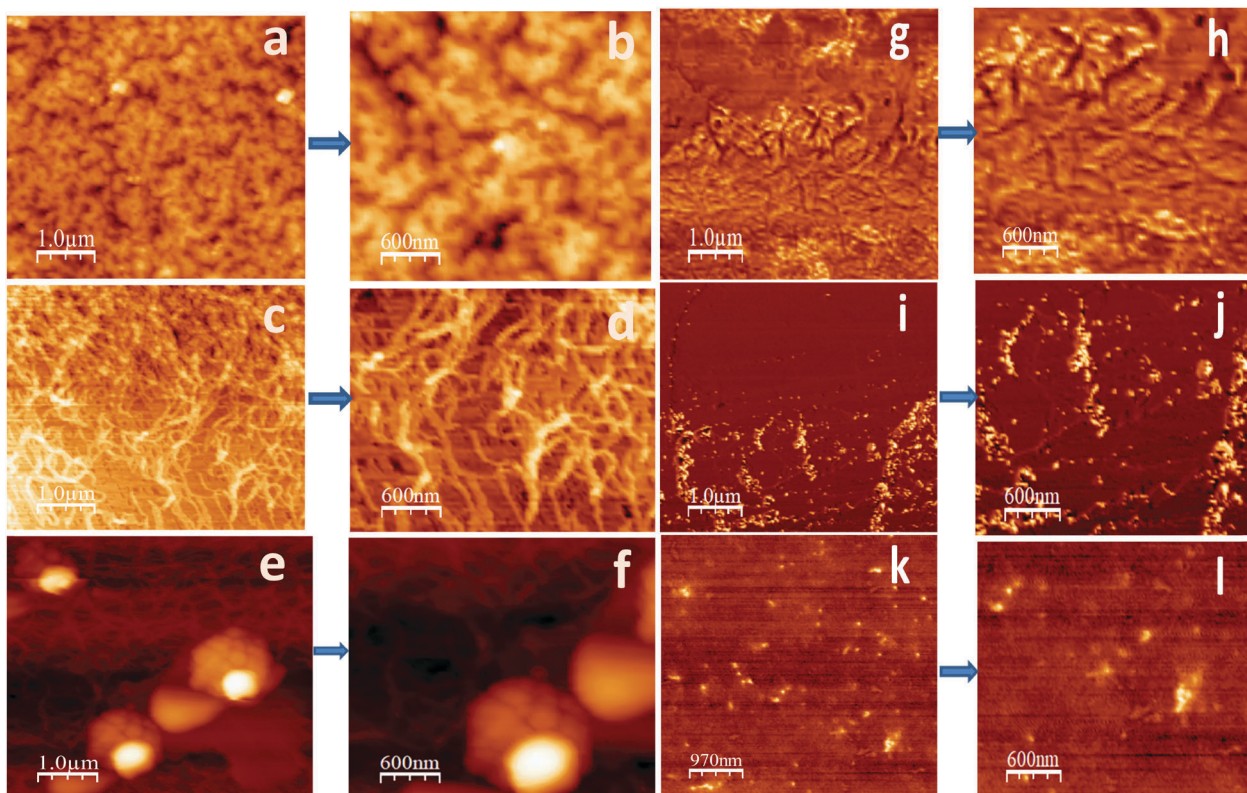


Fig. 7 FTIR spectra of native  $\beta$ -lg (profile a) and  $\beta$ -lg incubated at  $75^\circ\text{C}$  for 6 h in the absence (profile b) and presence of curcumin (profile c, profile d), DAC (profile e, profile f), IOC (profile g, profile h), PY (profile i, profile j) at molar concentration ratios of 1:0.5 and 1:1, respectively in 10 mM phosphate buffer at  $\text{pH} 7.4$  containing 2% ethanol. Protein concentrations were  $1087 \mu\text{M}$ . FTIR spectra were taken in the amide-I region of 1500 to  $1700 \text{ cm}^{-1}$ . Each spectrum is an average of 32 scans in  $\text{D}_2\text{O}$  solvent at  $25^\circ\text{C}$ .



**Fig. 8** AFM images representing the aggregate morphologies of  $\beta$ -lg in the presence of curcumin derivatives.  $\beta$ -lg (543  $\mu$ M) was co-incubated with equimolar concentrations of curcumin, DAC, IOC and PY for 24 h. Representative AFM images of  $\beta$ -lg aggregates (a) alone for 6 h [(b) zoomed-in image of (a)] and (c) for 24 h [(d) zoomed-in image of (c)] and co-incubated with (e) curcumin [(f) zoomed-in image of (e)], (g) DAC [(h) zoomed-in-image of (g)], (i) IOC [(j) zoomed-in image of (i)] and (k) PY [(l) zoomed-in image of (k)] for 24 h.

into smaller fragments, and the extent of fibril formation was diminished in the presence of DAC. However, in the case of IOC, higher order oligomeric structures were incorporated with small oligomers (Fig. 8, image i). Interestingly, PY promoted complete disruption of  $\beta$ -lg fibrils into smaller oligomers with unique morphologies (Fig. 8, image k).

### Docking study

A molecular docking study was performed to obtain insight into the types of interactions involved between  $\beta$ -lg and curcumin-stacking and  $\pi$ -interactions with Trp<sub>19</sub> and Tyr<sub>20</sub>, Tyr<sub>20</sub> and Glu<sub>44</sub> and Glu<sub>158</sub>, respectively (Fig. 9, image c). PY binds derivatives, which is responsible for the inhibition of aggregation. When the 1,3-dicarbonyl moiety was retained in DAC and was substituted by isoxazole and pyrazole, alterations in the inhibitory effects of curcumin were observed; DAC exhibited fewer inhibitory effects than curcumin, and PY showed superior inhibitory effects compared to IOC and DAC. The anti-amyloidogenic activity of curcumin can be attributed to its phenolic and polycyclic structure, which results in the formation of one hydrogen bond of the carbonyl of the  $\beta$ -diketone moiety of curcumin with  $\beta$ -lg accompanied by weak forces (Fig. 9, image a). The molecular docking results indicated that weak electrostatic interactions are favored by DAC (Fig. 9, image b). However, substitution in the  $\beta$ -diketone moiety of curcumin increased the anti-aggregation

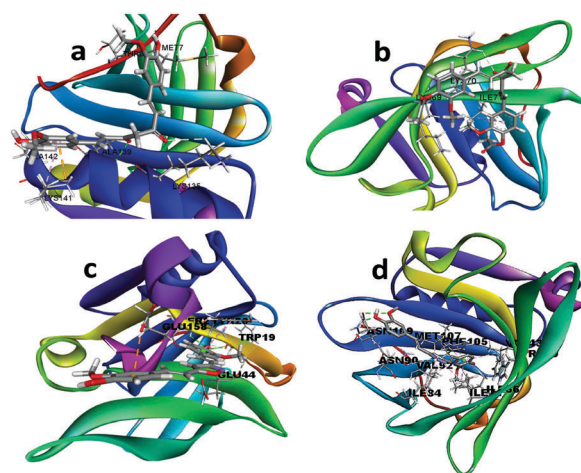


**Fig. 9** The structures of the most stable (a)  $\beta$ -lg-curcumin, (b)  $\beta$ -lg-DAC, (c)  $\beta$ -lg-IOC and (d)  $\beta$ -lg-PY complexes obtained by molecular docking, and possible interactions contributing to the binding (PDB ID of  $\beta$ -lg: 1BSY).

potential. The compound IOC prefers surface binding through H-bonding,  $\pi$ -stacking and  $\pi$ -interactions with Trp<sub>19</sub> and Tyr<sub>20</sub>, Tyr<sub>20</sub>, and Glu<sub>44</sub> and Glu<sub>158</sub>, respectively (Fig. 9, image c). Meanwhile, PY binds inside the calyx and interacts with the amino acids Val<sub>43</sub>, Ile<sub>56</sub>, Ile<sub>84</sub>, Asn<sub>90</sub>, Val<sub>92</sub>, Met<sub>107</sub>, Phe<sub>105</sub> and

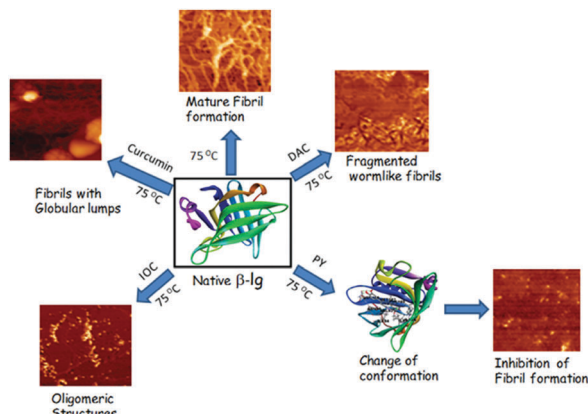


Fig. 10 Schematic representation of this work.

Asn<sub>109</sub> through  $\pi$ -interactions,  $\pi$ -stacking and H-bonding, respectively (Fig. 9, image d). The main interaction forces between  $\beta$ -lg and PY are hydrophobic interactions and aromatic stacking; these contribute to the binding of this compound to the intermediate structure of  $\beta$ -lg, stabilizing it and finally suppressing amyloid formation. Moreover, it was demonstrated that aliphatic residues such as alanine and valine present in the central region of protein facilitated the binding of more than one derivative to the protein, preventing interactions between monomers and retarding the overall aggregation process.<sup>18</sup> Thus, amino acids with aliphatic side chains in  $\beta$ -lg can also serve as binding sites for the aforementioned curcumin derivatives; this may be a mechanism by which these compounds decrease aggregation of  $\beta$ -lg (Fig. 10).

## Experimental

### Reagents and chemicals required

Bovine  $\beta$ -lg was isolated and purified from cow milk as described earlier.<sup>36</sup> The final product was lyophilized and stored at 4 °C. Sodium dihydrogen phosphate was purchased from Merck (Mumbai, India). Curcumin and different fluorescent probes, *viz.*, 8-anilinoanthralene-1-sulfonic acid ammonium salt (ANS), Congo red (CR) and Thioflavin T (ThT), were obtained from Sigma Chemical Co. (St. Louis, USA) and used as received without further purification. IOC and PY were synthesized according to previously described methods.<sup>37</sup> DAC was synthesized according to a previously described method<sup>38</sup> and further characterized by <sup>1</sup>H-NMR spectroscopy, <sup>13</sup>C-NMR spectroscopy and ESI-MS (all spectral data are given in SI3–SI5, ESI<sup>†</sup>). The other chemicals used were of the highest purity available.

### Preparation of $\beta$ -lg solution

For spectroscopic sample preparation,  $\beta$ -lg was weighed and dissolved in 0.01 M pH 7.4 phosphate buffer solution containing 2% ethanol. Protein stock solutions were prepared using phosphate buffer at pH 7.4. Because the extinction coefficient of  $\beta$ -lg ( $0.96 \text{ mg}^{-1} \text{ mL}^{-1} \text{ cm}^{-1}$  at 280 nm) is known, different

concentrations of protein samples were prepared by dissolving  $\beta$ -lg samples in Milli-Q water and then measuring the O.D. at 280 nm.

### Preparation of solutions of curcumin derivatives

The concentrations of curcumin and the IOC, PY and DAC derivatives were determined spectroscopically. The solutions of the derivatives were obtained by dissolving them in absolute ethanol to give concentrations of  $1 \times 10^{-3} \text{ M}$ .

### Thermal aggregation assay of $\beta$ -lg

Bovine  $\beta$ -lg readily undergoes aggregation upon thermal exposure at 75 °C when  $163 \mu\text{M}$  ( $3 \text{ mg mL}^{-1}$ ) of  $\beta$ -lg is used.<sup>39,40</sup> Thus, all the experiments were carried out upon thermal co-incubation of  $\beta$ -lg at 75 °C in the presence of curcumin and its derivatives (IOC, PY and DAC) at molar concentration ratios of 1:0.5 and 1:1 for 6 h. Each sample was freshly prepared and filtered through Sartorius filter paper (pore size 0.20  $\mu\text{m}$ ).

## Methods

### Electrophoresis measurements

Sodium dodecyl sulphate-polyacrylamide gel electrophoresis (SDS-PAGE) was performed under non-reducing conditions using 12% acrylamide resolving gel according to Laemmli's method.<sup>41</sup> Samples of  $\beta$ -lg solution ( $163 \mu\text{M}$ ) in 10 mM sodium phosphate buffer, pH 7.4, were incubated at 75 °C for 6 h in the absence and presence of curcumin and its derivatives (IOC, PY and DAC) separately at molar concentration ratios of 1:0.5 and 1:1. The resulting solutions were filtered with a syringe filter with a 0.2  $\mu\text{m}$  membrane filter. The sample solutions were mixed with equal amounts of SDS-gel loading solution and boiled at 95 °C to 100 °C before the SDS-PAGE analysis. Aliquots (20  $\mu\text{L}$ ) of thermally incubated  $\beta$ -lg solution in the presence and absence of curcumin derivatives were loaded in the wells. Similarly, 20  $\mu\text{L}$  of native  $\beta$ -lg solution ( $108 \mu\text{M}$ ) were loaded in another well. Electrophoretic separations were performed by applying a maximum voltage of 100 volts for 1 h. The gel was stained with Coomassie Brilliant Blue R-250 and destained by the usual method using a solution containing methanol and acetic acid.

### Intrinsic fluorescence

Intrinsic fluorescence measurements of all the above-described protein solutions were performed in Na-phosphate buffer, pH 7.4, containing 2% ethanol on a Shimadzu spectrofluorimeter (Shimadzu 5301 PC). The temperature was maintained at 25 °C. The fluorescence spectra were measured using a 1 cm path-length rectangular quartz cell while maintaining a  $\beta$ -lg concentration of  $13.6 \mu\text{M}$ . To monitor the intrinsic fluorescence of  $\beta$ -lg, the samples were excited at 295 nm and the spectra were recorded between 310 nm and 400 nm. The excitation and emission slits were set at 3 nm and 5 nm, respectively. All the experiments were performed at least three times.

### ANS fluorescence study

Exposure of hydrophobic patches in the protein during the aggregation process was monitored using the polarity-sensitive fluorescent probe 1-anilinonaphthalene-8-sulfonate (ANS).<sup>42</sup> A stock solution of ANS was added to each aliquot of  $\beta$ -lg solution (both in the absence and presence of curcumin and curcumin derivatives) so that the final ANS concentration in each aliquot was 30  $\mu$ M. Typically, the ANS concentration was 50 molar in excess of the protein concentration. The ANS-fluorescence intensities were measured using a Shimadzu RF-5301 PC instrument with excitation at 370 nm and by scanning the emission wavelength from 400 nm to 650 nm.<sup>43</sup> Slit widths were set at 3 nm for excitation and 5 nm for emission, respectively. Each spectrum was blank corrected. Data points were the average of triplicate measurements.

### Thioflavin T (ThT) binding assay

ThT is a dye which shows enhanced fluorescence at around 485 nm when bound to amyloid fibrils.<sup>44</sup> Thus, to investigate and compare the aggregates formed by thermally incubated  $\beta$ -lg in the absence and presence of curcumin and curcumin derivatives, the following assays were employed. A 5 mM stock solution of ThT was prepared in 20 mM sodium phosphate buffer, pH 7.5, and filtered through a 0.2  $\mu$ m polyether sulfone filter. A solution containing 50  $\mu$ L of 163  $\mu$ M  $\beta$ -lg sample [incubated in the absence and presence of curcumin derivatives for 6 h at molar concentration ratios of 1:1] was diluted in 950  $\mu$ L of 50  $\mu$ M ThT (dissolved in 0.01 M pH 7.4 phosphate buffer solution containing 2% ethanol) and incubated for 30 min at 25  $^{\circ}$ C in the dark. The resulting ThT fluorescence intensities of the samples were measured at each time point at an emission wavelength of 485 nm using an excitation wavelength of 440 nm. The percent change in fluorescence intensity (Fp) was calculated using eqn (1):

$$F_p = \left( \frac{F_t - F_0}{F_0} \right) \times 100 \quad (1)$$

where  $F_t$  is the fluorescence at a specific time point and  $F_0$  is the fluorescence at the starting time of incubation. All experiments were performed in triplicate. Percent inhibition was calculated using eqn (2):

$$F_x = 100 - (100F_s \div F_c) \quad (2)$$

where  $F_x$  is the percent inhibition,  $F_s$  is the percent increase in fluorescence intensity in the presence of the compounds and  $F_c$  is the percent increase in the fluorescence intensity of  $\beta$ -lg alone. The slit widths for both the excitation and emission were maintained at 5 nm. Three replicates were performed, and the data were averaged.

### Rayleigh light scattering

The effects of curcumin and curcumin derivatives on the aggregation of thermally incubated  $\beta$ -lg were monitored by Rayleigh light scattering (RLS) measurements by observing the emission at 350 nm after exciting the solution at 350 nm using 10 mM

phosphate buffer at pH 7.4 containing 2% ethanol in a Shimadzu spectrofluorimeter (Shimadzu 5301 PC). The fluorescence spectra were collected at 25  $^{\circ}$ C using a 1 cm path length cell and a protein concentration of 13.6  $\mu$ M. The excitation and emission slits were set at 3 nm.

### Congo red assay

The formation of aggregates by thermally exposed  $\beta$ -lg in the absence and presence of curcumin and curcumin derivatives was investigated by measuring the shifts in the absorbance of Congo red in the region of 400 to 700 nm. Congo red stock solution (10 mM) was prepared by dissolving the dye in 10 mM sodium phosphate buffer (pH 7.0) containing 150 mM NaCl under continuous stirring. The solution was then filtered with a 0.2 mm Millipore filter. A fresh working solution was prepared by diluting the stock solution 100 times.<sup>45</sup> For this study, 250  $\mu$ L (27.2  $\mu$ M) aliquots of the protein solutions (containing curcumin and curcumin derivatives) were withdrawn and mixed with 250  $\mu$ L of a solution containing 40  $\mu$ M Congo red solution. The final volume (2 mL) was adjusted with 10 mM sodium phosphate buffer, pH 7.4, containing 2% ethanol.

### Analysis of secondary structures by CD spectroscopy

To trace the structural or conformational changes that curcumin and curcumin derivatives impose on  $\beta$ -lg, circular dichroism measurements (CD) were carried out on a Jasco spectropolarimeter (J-815) at 20  $^{\circ}$ C in the far-UV region (200 to 260 nm) using rectangular cells with 2 mm path lengths. Thermally incubated  $\beta$ -lg solutions (in the presence and absence of curcumin and curcumin derivatives) with concentrations of 13.6  $\mu$ M were used for the far-UV CD measurements. All the spectra are the average of three scans. The final spectrum was obtained after subtraction of the corresponding solvent spectrum. The far UV-CD curves were fitted with the curve-fitting software program CDNN 2.1 to determine the percentages of secondary structures present in  $\beta$ -lg under different conditions.

### Dynamic light scattering (DLS) measurements

The diffusion of particulates in solution induces fluctuations in the intensity of the scattered light. DLS detects these fluctuations using an auto-correlator on a microsecond time scale and is used to analyze the distribution of molecules and supramolecular aggregates because it is very sensitive to particle size.<sup>46</sup> Different sizes of molecules in the solution can be observed at different peaks if their sizes vary sufficiently. In our experiments, DLS measurements were performed with thermally incubated  $\beta$ -lg in the presence and absence of curcumin and curcumin derivatives employing a Zetasizer Nanos (Malvern Instrument, U.K.) equipped with a 633 nm laser and using a 2 mL rectangular cuvette (path length 10 mm). Measurements were performed at 20  $^{\circ}$ C with 250  $\mu$ L of coincubated  $\beta$ -lg sample in 1.75 mL Na-phosphate buffer. Then, the solutions were maintained for 30 minutes. Similar measurements were performed separately with the incubated  $\beta$ -lg in the absence of curcumin and curcumin derivatives.

The time-dependent auto correlation functions were acquired with twelve acquisitions for each run.

### Monitoring the secondary structural changes of $\beta$ -lg during thermal incubation by FTIR spectroscopy

For the FTIR measurements, native and incubated  $\beta$ -lg solutions (50  $\mu$ L) (in the presence and absence of curcumin and curcumin derivatives) with concentrations of 20 mg mL<sup>-1</sup> were taken in a Microcon filter device and diluted with 200  $\mu$ L of D<sub>2</sub>O. The mixture was then quickly centrifuged at 4000  $\times g$  for 8 min until the volume reached  $\sim$ 50  $\mu$ L. After that, 200  $\mu$ L of D<sub>2</sub>O was added again, and the mixture was centrifuged for another 8 to 10 minutes. This process of D<sub>2</sub>O exchange was repeated 3 to 4 times.<sup>47</sup> Finally, the D<sub>2</sub>O-exchanged  $\beta$ -lg samples were placed between two CaF<sub>2</sub> windows separated by a 50  $\mu$ M thick Teflon spacer. FTIR scans were collected in the range of 1500 to 1700 cm<sup>-1</sup> at a resolution of 2 cm<sup>-1</sup> in a N<sub>2</sub> environment using a Spectrum 100 FT-IR spectrometer (Perkin Elmer). The spectrum of D<sub>2</sub>O at pD 7.5 was collected and subtracted from the sample spectrum.

### Atomic force microscopy (AFM)

AFM was used to monitor the effects of curcumin and curcumin derivatives on  $\beta$ -lg fibril formation. For AFM analysis, the protein samples were diluted to 0.2 mg mL<sup>-1</sup> in buffer, and 10  $\mu$ L of each sample was placed on a piece of mica (1 cm  $\times$  1 cm pieces). The AFM samples were dried at room temperature and then used to acquire the AFM images. The AFM images were recorded using a VEECO DICP II autoprobe (Model AP 0100) instrument.

### Molecular docking study of $\beta$ -lg-curcumin derivative interactions

The molecular docking study was performed using Autodock 4.2 and Autodock Tools (ADT) using a Lamarckian genetic algorithm. The crystal structure of  $\beta$ -lg (PDB ID: 1BSY) was obtained from the RCSB Protein Data Bank. The structures of curcumin, DAC, IOC and PY were optimized to lower energies using density functional theory (DFT) at the B3LYP/6-31G level of theory. These optimized structures were used for docking with  $\beta$ -lg to predict the binding sites and modes of binding. For the docking study, ligands present in the protein (1BSY) and water molecules were removed from the protein, and atom Kollman charges were assigned after the addition of polar hydrogen to the protein. The protein was set to be rigid, and there was no consideration of solvent molecules on docking. Discovery Studio 4.1 Client and Chimera 1.10.1rc were used for visualization effects and to identify the residues involved in binding.

## Conclusions

To conclude, our current study demonstrates that among the aforementioned curcumin derivatives, PY is a potent therapeutic molecule that can be used in stoichiometric amounts to suppress the fibril formation of  $\beta$ -lg by exploration of various biophysical

and imaging tools, including SDS-PAGE, ThT fluorescence, ANS binding, CD measurements, DLS, RLS, FTIR and AFM. In summary, these four curcuminoids can prevent aggregation of the protein and its toxic intermediates *via* different moieties of the curcuminoid framework, such as the  $\beta$ -diketone moiety, phenolic OH groups, acetyl groups, hepta-diene moiety, substitutions on the benzene nucleus and substitutions on the  $\beta$ -diketone moiety. Alternatively, it can be suggested that curcumin analogs also directly bind to fibrillar assemblies in a similar fashion, but more efficiently than curcumin, and disrupt preformed fibrils. Overall, our data revealed the efficacy of the compounds in the order of PY > IOC > DAC > curcumin. The adoption of a helical intermediate and the formation of nonfibrillar aggregates in the presence of PY may be a feature to exploit for structural investigations in molecular docking studies. The hypothesis of protein association into dimers aided by the PY derivative was further supported by SDS-PAGE studies and DLS measurements of protein solutions. Simultaneously, these measurements excluded the possibility of formation of higher rank linear aggregates. Hydrophobic interactions and hydrogen bonding between  $\beta$ -lg and PY are key forces implicated to play dominant roles in the inhibited activity. Curcumin pyrazole and its derivative *N*-(3-nitrophenylpyrazole) exhibited remarkable potency in arresting fibrillization and disrupting preformed fibrils of  $\alpha$ -synuclein.<sup>18</sup> The future projections of this study are to investigate the modulatory role of these molecules in drug formulations against disease progression in systemic amyloidosis and Alzheimer's disease.

## Conflicts of interest

The authors declare no competing financial interest.

## Acknowledgements

Financial support of University Grant Commission UGC-CAS-II and DST-PURSE-II (Govt of India) Program of Department of Chemistry, Jadavpur University, Kolkata are greatly acknowledged. The authors wish to acknowledge Prof. S. C. Bhattacharya, Department of Chemistry, Jadavpur University for providing the DLS instrumental facility. Sanhita Maity, SRF, is a recipient of UGC-NET Research Fellowship in Chemistry. AP acknowledges DST for funding through the INSPIRE program.

## Notes and references

- 1 I. M. Gonzalez and C. Soto, *Semin. Cell Dev. Biol.*, 2011, **22**, 482.
- 2 N. Stefanova, P. Bucke, S. Duerr and G. K. Wenning, *Lancet Neurol.*, 2009, **8**, 1172.
- 3 M. R. H. Krebs, L. A. Morozova-Roche, K. Daniel, C. V. Robinson and C. M. Dobson, *Protein Sci.*, 2004, **13**, 1933.
- 4 Alzheimer's Association, *Alzheimer's Dementia*, 2013, **9**, 208.
- 5 C. Ballard, S. Gauthier, A. Corbett, C. Brayne, D. Aarsland and E. Jones, *Lancet*, 2011, **377**, 1019.

- 6 J. D. Grill and J. L. Cummings, *Expert Rev. Neurother.*, 2010, **10**, 711.
- 7 R. Anand, K. D. Gill and A. A. Mahdi, *Neuropharmacology*, 2014, **76**, 27.
- 8 K. Chiang and E. H. Koo, *Annu. Rev. Pharmacol. Toxicol.*, 2014, **54**, 381.
- 9 W. S. Gosal, A. H. Clark, P. D. A. Pudney, B. Simon and R. Murphy, *Langmuir*, 2002, **18**, 7174–7181.
- 10 M. J. Volles, S. J. Lee, J. C. Rochet, M. D. Shtilerman, T. T. Ding, J. C. Kessler and J. P. T. Lansbury, *Biochemistry*, 2001, **40**, 7812.
- 11 L. Pieri, K. Madiona, L. Bousset and R. Melki, *Biophys. J.*, 2012, **102**, 2894.
- 12 M. N. Shinde, N. Barooah, A. C. Bhasikuttan and J. Mohanty, *Chem. Commun.*, 2016, **52**, 2992.
- 13 A. C. Bhasikuttan and J. Mohanty, *Chem. Commun.*, 2017, **53**, 2789.
- 14 M. N. Shinde, R. Khurana, N. Barooah, A. C. Bhasikuttan and J. Mohanty, *J. Phys. Chem. C*, 2017, **121**, 20057.
- 15 B. Bohrmann, M. Adrian, J. Dubochet, P. Kuner, F. Müller, W. Huber, C. Nordstedt and H. Dobeli, *J. Struct. Biol.*, 2000, **130**, 232.
- 16 E. N. Lee, H. J. Cho, C. H. Lee, D. Lee, K. C. Chung and S. R. Paik, *Biochemistry*, 2004, **43**, 3704.
- 17 B. C. H. May, A. T. Fafarman, S. B. Hong, M. Rogers, L. W. Deady, S. B. Prusiner and F. E. Cohen, *Proc. Natl. Acad. Sci.*, 2003, **100**, 3416.
- 18 B. Cheng, H. Gong, H. Xiao, R. B. Petersen, L. Zheng and K. Huang, *Biochim. Biophys. Acta*, 2013, **1830**, 4860.
- 19 S. Rigacci, V. Guidotti, M. Bucciattini, D. Nichino, A. Relini, A. Berti and M. Stefani, *Curr. Alzheimer Res.*, 2011, **8**, 841.
- 20 P. Yoyungnoen, P. Wirachwong, C. Changtam, A. Suksamrarn and S. Patumraj, *World J. Gastroenterol.*, 2008, **14**, 2003.
- 21 N. Ahsan, S. Mishra, M. K. Jain, A. Surolia and S. Gupta, *Sci. Rep.*, 2015, **5**, 9862.
- 22 Q. Xu, D. Yuhong, L. Bin, Z. Yinglin, S. Weiyan, H. Yingpeng, H. Jianing, Y. Yanjun, Z. Binhua, D. Jun, F. Haiyan and B. Xianzhang, *J. Med. Chem.*, 2010, **53**, 8260.
- 23 A. S. Pithadia, A. Bhunia, R. Sribalan, V. Padmini, C. A. Fierkeac and A. Ramamoorthy, *Chem. Commun.*, 2016, **52**, 942.
- 24 M. Z. Papiz, L. Sawyer, E. E. North, A. C. Findlay, J. B. Sivaprasadarao, R. Jones, T. A. Newcomer and M. E. Kraulis, *Nature*, 1986, **324**, 383.
- 25 T. V. Burova, Y. Choiset, V. Tran and T. Haertle, *Protein Eng.*, 1998, **11**, 1065.
- 26 Z. Teng, R. Xua and Q. Wang, *RSC Adv.*, 2015, **5**, 35138.
- 27 E. H. C. Bromley, M. R. H. Krebs and A. M. Donald, *Eur. Phys. J. E: Soft Matter Biol. Phys.*, 2006, **21**, 145.
- 28 D. E. Dunstan, P. H. Brown, P. Asimakis, W. Duckera and J. Bertolini, *Soft Matter*, 2009, **5**, 5020.
- 29 L. Bateman, A. Ye and H. Singh, *J. Agric. Food Chem.*, 2011, **59**, 9605–9611.
- 30 M. A. M. Hoffmann and P. J. J. M. Van Mil, *J. Agric. Food Chem.*, 1997, **45**, 2942.
- 31 S. Ikeda and V. J. Morris, *Biomacromolecules*, 2002, **3**, 382–389.
- 32 B. Ma, J. Xie, L. Wei and W. Li, *Int. J. Biol. Macromol.*, 2013, **53**, 82.
- 33 V. Bellotti, P. Mangione and G. Merlini, *J. Struct. Biol.*, 2000, **130**, 280.
- 34 R. Narlawar, M. Pickhardt, S. Leuchtenberger, K. Baumann, S. Krause, T. Dyrks, S. Weggen, E. Mandelkow and B. Schmidt, *ChemMedChem*, 2008, **3**, 165.
- 35 S. Chakraborti, G. Dhar, V. Dwivedi, A. Das, A. Poddar, G. Chakraborti, G. Basu, P. Chakrabarti, A. Surolia and B. Bhattacharyya, *Biochemistry*, 2013, **52**, 7449.
- 36 J. Chakraborty, N. Das, K. P. Das and U. C. Halder, *Int. Dairy J.*, 2009, **19**, 43.
- 37 S. Maity, S. Pal, S. Sardar, N. Sepay, H. Parvej, J. Chakraborty and U. C. Halder, *RSC Adv.*, 2016, **6**, 112175.
- 38 F. Mohammadi, A. K. Bordbar, A. Divsalar, K. Mohammadi and A. A. Saboury, *Protein J.*, 2009, **28**, 117.
- 39 R. N. Zuniga, A. Tolkach, U. Kulozik and J. M. Aguilera, *J. Food Sci.*, 2010, **75**, 261.
- 40 M. R. H. Kerbs, G. L. Derlin and A. M. Donald, *Biophys. J.*, 2009, **96**, 5013.
- 41 U. K. Laemmli, *Nature*, 1970, **227**, 680.
- 42 G. V. Semisotnov, N. A. Radionava, O. I. Razgulyaev, V. N. Uversky, A. F. Gripas and R. I. Gilmanshin, *Biopolymers*, 1991, **31**, 119.
- 43 J. M. Khan, A. Qadeer, E. Ahmad, R. Ashraf, B. Bhushan, S. K. Chaturvedi, G. Rabbani and R. H. Khan, *PLoS One*, 2013, **8**, 62428.
- 44 M. R. Nilsson, *Methods*, 2004, **34**, 151.
- 45 S. A. Hudson, H. Ecroyd, T. W. Kee and J. A. Carver, *FEBS J.*, 2009, **276**, 5960.
- 46 W. W. Yu, E. Chang, J. C. Falkner, J. Zhang, A. M. S. Somali, C. M. Sayes, J. Johns, R. Drezek and V. L. Colvin, *J. Am. Chem. Soc.*, 2007, **129**, 2871.
- 47 V. Bannerjee and K. P. Das, *Colloids Surf., B*, 2012, **92**, 142.
- 48 G. A. Manderson, M. J. Handmann and L. K. Creamer, *J. Agric. Food Chem.*, 1998, **46**, 5052.
- 49 T. Croguennee, B. T. O'Kennedy and R. Mehra, *Int. Dairy J.*, 2004, **14**, 399.
- 50 S. H. Mousavi, A. K. Bordbar and T. Haertle, *Protein Pept. Lett.*, 2008, **15**, 818.
- 51 B. J. Harvey, E. Bell and L. Brancaleon, *J. Phys. Chem. B*, 2007, **111**, 2610.
- 52 E. Schonbrunn, S. Eschenburg, K. Luger, W. Kabsch and N. Amrhein, *Proc. Natl. Acad. Sci.*, 2000, **97**, 6345.
- 53 L. Styrrer, *J. Mol. Biol.*, 1965, **13**, 482.
- 54 R. N. Zuniga, A. Tolkach, U. Kulozik and J. M. Aguilera, *J. Food Sci.*, 2010, **75**, 261.
- 55 S. A. Hudson, H. Ecroyd, T. W. Kee and J. A. Carver, *FEBS J.*, 2009, **276**, 5960.
- 56 A. Shpigelman, G. Israeli and Y. D. Livney, *Food Hydrocolloids*, 2010, **24**, 735.
- 57 S. Maity, S. Sardar, S. Pal, H. Parvej, J. Chakraborty and U. C. Halder, *RSC Adv.*, 2016, **6**, 74409.
- 58 H. Thurow and K. Geisen, *Diabetologia*, 1984, **27**, 212.
- 59 S. Sardar, S. Pal, S. Maity, J. Chakraborty and U. C. Halder, *Int. J. Biol. Macromol.*, 2014, **69**, 137.